



This is a repository copy of *Wear of driving versus driven discs in a twin disc rolling-sliding test*.

White Rose Research Online URL for this paper:

<https://eprints.whiterose.ac.uk/196919/>

Version: Published Version

Article:

Hu, Y., Wang, W.J., Watson, M. et al. (4 more authors) (2023) Wear of driving versus driven discs in a twin disc rolling-sliding test. *Wear*, 512-513. 204528. p. 204528. ISSN 0043-1648

<https://doi.org/10.1016/j.wear.2022.204528>

Reuse

This article is distributed under the terms of the Creative Commons Attribution (CC BY) licence. This licence allows you to distribute, remix, tweak, and build upon the work, even commercially, as long as you credit the authors for the original work. More information and the full terms of the licence here:

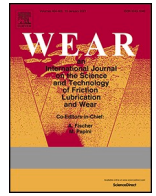
<https://creativecommons.org/licenses/>

Takedown

If you consider content in White Rose Research Online to be in breach of UK law, please notify us by emailing eprints@whiterose.ac.uk including the URL of the record and the reason for the withdrawal request.



eprints@whiterose.ac.uk
<https://eprints.whiterose.ac.uk/>



Wear of driving versus driven discs in a twin disc rolling-sliding test

Y. Hu^a, W.J. Wang^b, M. Watson^c, K. Six^d, H. Al-Maliki^d, A. Meierhofer^d, R. Lewis^{c,*}

^a Aviation Engineering College, Civil Aviation Flight University of China, Guanghan, 618307, China

^b Tribology Research Institute, State Key Laboratory of Traction Power, Southwest Jiaotong University, Chengdu, 610031, China

^c Department of Mechanical Engineering, The University of Sheffield, Mappin Street, Sheffield, S1 3JD, UK

^d Virtual Vehicle Research GmbH, Graz, Austria

ARTICLE INFO

Keywords:

Driving
Driven
Wear mechanism
Stress state

ABSTRACT

Theoretically, the stress states in wheel and rail will be different during braking (rail driving) and acceleration (wheel driving), and this will lead to different wear mechanisms and rates in each. In order to reveal the wear mechanism of wheel and rail materials under these different conditions, existing twin disc work on the wear and damage of wheel and rail where they were both considered was analysed. Some trends emerged, but there was little consistency in the way the different tests had been conducted. To avoid hardness/microstructure variables, new tests were then outlined where the same material pairs were used. The results indicated that the wear rate of the driving disc (faster one) was significantly higher than that of the driven one. The driven discs mainly experienced fatigue and abrasion mechanisms, while the driving one more typically suffered tribo-chemical reactions and fatigue. Finally, the potential causes for the difference in wear behaviours between the driving and driven discs were identified: the hardness; the formation mechanism of metal debris; the stress state; the material properties and the varying work conditions. This work has provided some important new data on wear trends at different driving conditions that will be helpful in the subsequent modelling of wheel and rail wear.

1. Introduction

The wheel-rail pair is one of the core components in a railway system. The service behaviour of wheel and rail can affect the safety of a railway vehicle, ride comfort and the maintenance costs [1]. In order to reduce damage of wheels and rails, numerous studies have been conducted based on the severe wear and rolling contact fatigue (RCF) mechanisms occurring at the wheel-rail interface, including theoretical analysis [2,3], field surveys and laboratory tests [4]. However, no unified and clear wear mechanisms have been established so far. The main reason is that the wheel-rail contact interface is in a complex multi-axial alternating stress state, resulting in variable damage and degradation mechanisms [5]. Temperature is also influential, particularly at high creepage levels. Correspondingly, the establishment of wear models and the implementation of accurate life predictions have become extremely difficult. A more realistic prediction of the wear of wheel and rail requires further data for wear rates for each scenario.

The widely performed twin disc test in wheel-rail wear research typically gives creepages via the setting of a speed difference between two small-sized discs [4]. When the wheel disc is faster, it is defined as a positive creepage, which simulates accelerating conditions; otherwise, it

is negative creepage, simulating braking conditions. In this paper, the faster disc in a twin disc test is defined as the “driving” disc, while the relatively slow disc is defined as the “driven” one. Theoretically, the stress states in a wheel and rail will be different during braking (rail runs faster) and acceleration (wheel runs faster) and this will lead to different wear mechanisms and rates in each. However, little research has been focused on such differences between the driving and driven discs.

Deters et al. [6] have carried out the most comprehensive study on this issue. They ran a series of twin disc tests under both accelerating and braking conditions, the results are shown in Fig. 1. At high creepage ($\geq \pm 1\%$), the wheel wear is generally higher than the rail when either disc is driving, the authors concluded that this was due to the wheel disc material being generally softer post work hardening. Besides, the 900A rail is also harder than the R7 wheel before testing. The softer material is generally believed to wear more in a twin disc test [7]. Therefore, it is difficult to reveal the influence of driving states on wear mechanisms from this result.

However, the above difference in wear and hardness is only obvious at relatively high creepages, indicating that the wear mechanism of the driving and driven discs is related to contact conditions in the twin disc test. Notably, at low positive creepages of less than 0.25%, the wear

* Corresponding author.

E-mail address: roger.lewis@sheffield.ac.uk (R. Lewis).

<https://doi.org/10.1016/j.wear.2022.204528>

Received 24 June 2022; Received in revised form 15 September 2022; Accepted 13 October 2022

Available online 18 October 2022

0043-1648/© 2022 The Authors. Published by Elsevier B.V. This is an open access article under the CC BY license (<http://creativecommons.org/licenses/by/4.0/>).

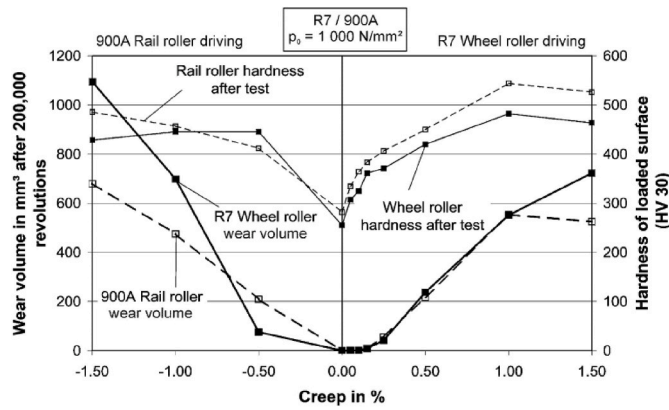


Fig. 1. Wear volume and hardness as a function of creepage [6].

mechanism of wheel and rail discs is described as “tribo-chemical” wear, because both driving and driven discs were completely covered with a reddish-brown and shiny oxide layer (note that very low negative creepages tests were not performed). This tribo-chemical phenomenon at low creepages has also been seen by Lewis et al. and in the field on both wheels and rails [8]. Whereas, as the creepage increased, the wear mechanism changed to a fatigue and abrasion mechanism for the driven disc (slower one) and tribo-chemical reaction and fatigue for the driving disc (faster one).

The above discussion suggests that there are different wear mechanisms in the driving and driven discs. However, more examination of these mechanisms is needed to provide a more comprehensive explanation of what is happening in the two discs. The wear data and improved understanding of the wear mechanisms can be used to improve modelling of wheel and rail wear, especially more specific wear rates for braking and accelerating periods.

The aim of this work was to collate existing data where, for the same material pairs, the wheel disc has been run driving and driven to see what the emerging trends are. Within existing data, wheel and rail vary between being driving and driven, and unfortunately no studies look at both situations using the same wheel and rail materials. As a result, in the first section of this paper the effects are studied in terms of hardness ratio between wheel and rail materials rather than specific materials. In the second part of the work new tests are outlined where the same material pairs are used to understand mechanisms better. The purpose of using the same materials is to avoid hardness/microstructure variables.

2. Analysis of data from previous studies

The first stage of this work was focused on looking at data in the literature to see what trends emerge as wheel discs were run in driving and driven situations. As mentioned previously, there is little data available where this has been done using the same material pair. To try

and find a way around this problem, material pairs were considered by hardness ratio H_R/H_W (rail hardness, H_R divided by wheel hardness, H_W , here both H_R and H_W were the hardness before tests). Given the differences in specimen geometries and contact stresses used, the wear was plotted against $T\gamma/A$, where T is tractive force (normal force \times friction), γ is creepage and A is contact area (in mm^2). This is a common means of translating wear rates generated in small scale laboratory test-rigs to the full sized wheel/rail interface [4,5].

Fig. 2 shows the wear rate and the wheel/rail wear ratio (W_W/W_R) for the same wheel-rail pairs (CL60-U75V) (with a H_R/H_W of 0.975 (pre-test hardness values)) as a function of $T\gamma/A$ in both cases where the wheel and rail materials were run driving, results were obtained via twin disc tests carried out at the Southwest Jiaotong University. Fig. 2a shows that in the two driving modes, the wheel and rail wear rates tend to increase with increasing $T\gamma/A$. However, at the same $T\gamma/A$ condition, the wear rate values for CL60 wheel and U75V rail under the two driving modes are not exactly the same. These differences can be not only attributed to which material was run driving, but it will also be related to the different test rigs used and different test cycles (WR-1 rig and 180,000 cycles for the case where the U75V rail was driving [9], MJP-30A and 25,000 cycles for the case where the CL60 wheel was driving [10]). Besides, Fig. 2b shows that W_W/W_R values are greater than 1 at almost all the $T\gamma/A$ conditions, so the CL60 wheel discs wear more than U75V rail discs for both driving cases.

In addition to the contact conditions ($T\gamma/A$), the material matching (H_R/H_W before tests) of the wheel-rail pair also affects the wear distribution in different driving modes. Fig. 3 shows previous results of wheel/rail hardness matching tests [11,12] with a similar $T\gamma/A$ condition together. Data in Fig. 3a comes from a twin disc study (MJP-30A rig, Southwest Jiaotong University) where the rail was run driving [11]. Five kinds of pearlitic wheels (ER7, ER8, CL60, C-class and D-class) and four kinds of pearlitic rails (U71Mn, U75V, PG4 and PG5) were cross-matched to get the H_R/H_W values of 0.7–1.6. It is clear from Fig. 3a that both the wheel and rail wear rates increase with the increasing H_R/H_W . Different from the data in Fig. 2, the W_W/W_R values are stable around 1.0, meaning that the driving disc (rail) wears at a similar rate to the driven one (wheel).

On the contrary, another twin disc study (Korea Railroad Research Institute, five kinds of wheel materials cross-matched with KS60 and KS60H rails) where the wheel was run driving [12] in Fig. 3b shows that with an increase in H_R/H_W , the wheel wear rates are nearly unchanged, while the rail wear rates decrease. W_W/W_R values increase with H_R/H_W , and the wheels (driving discs) wear more than the rails (driven discs) in the H_R/H_W values of 0.6–1.4.

The above analysis confirms that the wear rates of the discs absolutely are affected by driving modes. However, due to the complicated simulation conditions of the previous tests, the critical influencing mechanisms cannot be clearly revealed via the analysis of the wear rates only. Fig. 4 shows the worn surfaces of the driving and driven discs in different studies [6,13,14]. The observations for the same wheel-rail pairs (CL60-U75V) indicate that although the morphologies of the two

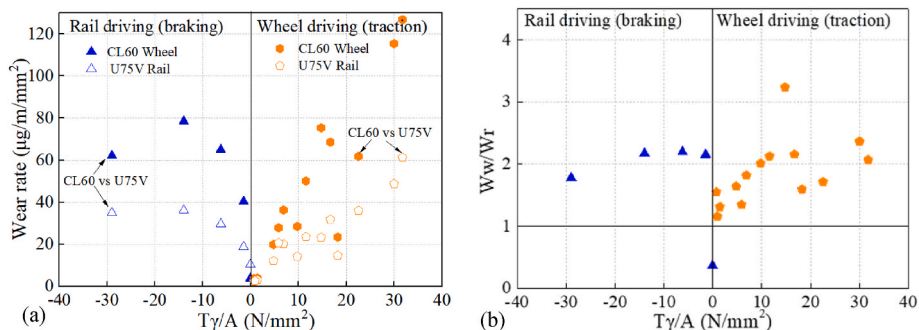


Fig. 2. (a) Wear rate and (b) wheel/rail wear ratio (W_W/W_R) for CL60-U75V pair in different driving conditions (line contact, data from Refs. [9,10]).

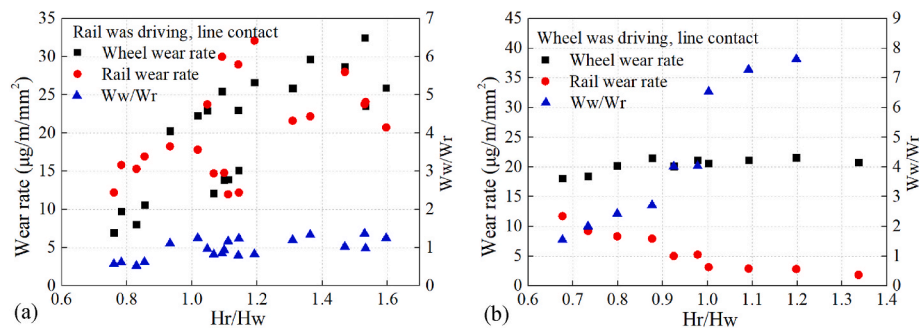


Fig. 3. Wear rate and W_w/W_r as a function of H_r/H_w (ratio of pre-test hardness values): (a) the rail was run driving at T_7/A values of 4.1–4.9 N/mm^2 (data from Ref. [11], 1500 MPa, 1.0%); (b) the wheel was run driving at T_7/A values of around 3.9 N/mm^2 (data from Ref. [12], 1100 MPa, 1.0%).

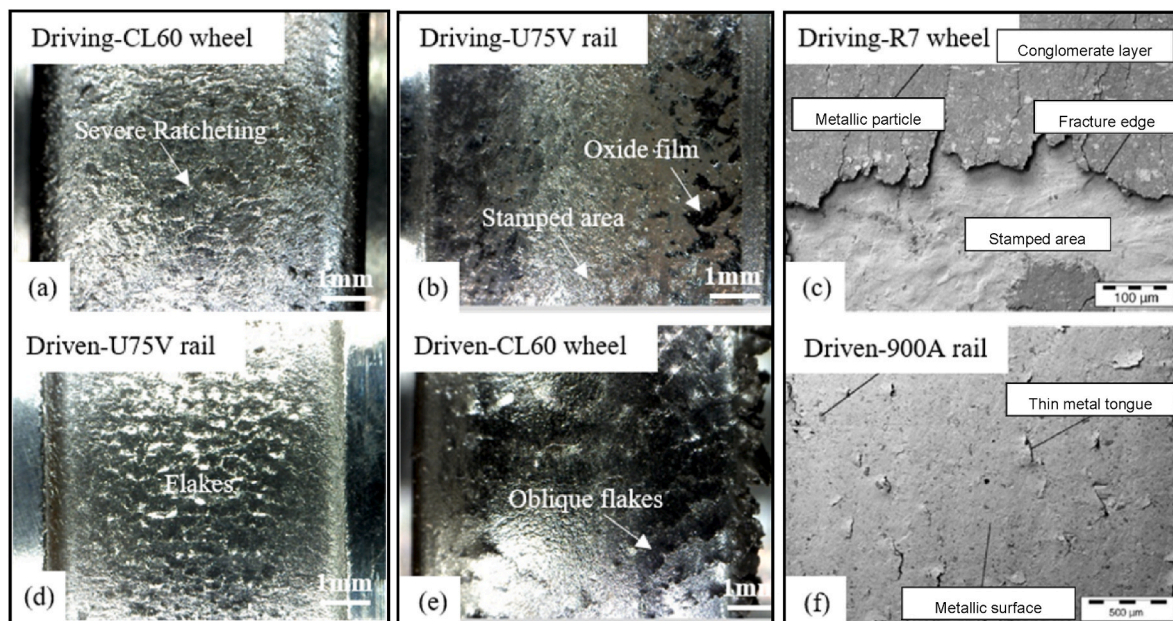


Fig. 4. Worn surfaces for different conditions: (a) and (d) are cited from Ref. [13] where the CL60 wheel was run driving and U75V rail was run driven for 50,000 cycles (MJP-30A rig, 1500 MPa, 1.5%); (b) and (e) come from Ref. [14] where the U75V rail was run driving and the CL60 wheel was run driven for 240,000 cycles (WR-1 rig, 850 MPa, 0.91%); (c) and (f) are derive from Ref. [6] when the R7 wheel was run driving.

discs vary under different contact conditions, oxide layer and ratcheting are typified in the driving discs (Fig. 4a and b), and flakes are dominating in the driven discs (Fig. 4d and e). This trend is totally consistent with the results of the twin disc tests performed by Deters et al. [6], as seen in Fig. 4c,f. Consequently, the wear mechanism for the driving disc is mainly tribo-chemical reactions and fatigue, while the driven disc is typified by fatigue and abrasion.

The difference in the wear mechanism of the driving and driven discs (see Fig. 4) would inevitably affect the wear and fatigue damage behaviours of wheel and rail. However, previous tests were performed under complex conditions [15–17], and the wear behaviours of wheel and rail are influenced by material matching (i.e., H_r/H_w) and working conditions (i.e., T_7/A), so that only analysing the previous results cannot fully clarify the damage mechanisms of the driving and driven discs. Therefore, it was necessary to perform further studies using the same material for both discs.

It is important to consider both the wear mechanisms and crack growth behaviour as how these interact is important. A wear failure is more acceptable than that caused by crack initiation and growth which in the worst case could lead to a rail break [18]. Therefore, it is desirable that there is enough wear to remove cracks. This could be through wear due to the wheel and rail interaction, or through artificial wear through grinding.

3. New twin disc testing

3.1. Experimental details

Two new series of wear experiments were performed using the SUROS twin disc rig (see Refs. [19,20] for full details) in the University of Sheffield and the WR-1 twin disc rig (see Ref. [9] for specific details) in Southwest Jiaotong University. Two discs were loaded together and run at the set rotational speeds to simulate a line contact between wheel and rail materials. The creepage required was achieved by adjustment of speeds. For the SUROS machine, the two discs are powered and controlled by independent AC motors, and the load is applied to the faster disc hydraulically. Concerning to the WR-1 rig, the faster disc is controlled by a DC motor and loaded mechanically, and the speed of the slower one is achieved by adjusting the transmission gear pair.

The discs used during the SUROS testing were cut from R260 rail heads. They were machined to a diameter of 47 mm with a contact width of 10 mm (Fig. 5a). The discs used during the WR-1 testing were taken from C-class wheel rims, and were processed into a diameter of 40 mm with a contact width of 5 mm (Fig. 5b). The chemical compositions and hardness values of the materials are exhibited in Table 1.

Both the SUROS and WR-1 wear tests were carried out in dry conditions using the same material pairs, the lower disc was run as the

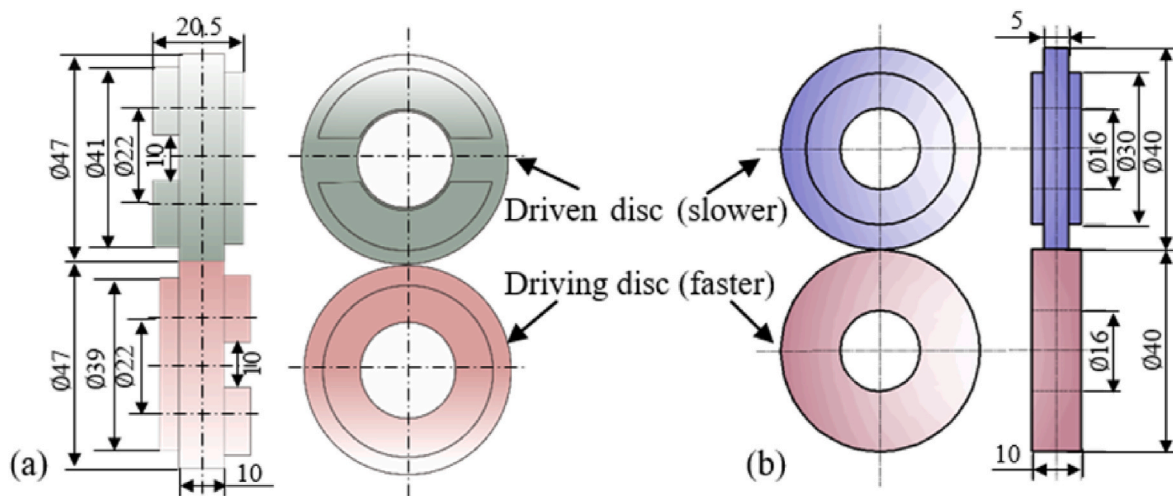


Fig. 5. Sample size: (a) SUROS tests; (b) WR-1 tests.

Table 1
Chemical compositions and hardness of the materials.

Type	Grade	Chemical composition (wt%)					Hardness/HV _{0.5}
		C	Si	Mn	P	S	
Rail	R260	0.62–0.80	0.15–0.58	0.70–1.20	≥0.025	≥0.025	287 ± 10
Wheel	C-class	0.67–0.77	0.15–1.00	0.60–0.90	0.030	0.005–0.040	388 ± 9

driving disc with a faster speed and the upper disc was run as the driven one, as shown in Fig. 5. The test conditions are shown in Table 2. The SUROS tests (Test 1~Test 3) were conducted at 400 rpm rotational speed, and stopped every 5000 cycles to observe the evolutions of wear rate and surface damage. After 40,000 cycles, the creepage was shifted to 0%, and tests were stopped every 500 cycles to see the responses of wear and damage for the driving and driven disc without further shear stress. During the testing, air cooling was provided to both discs, and wear debris was collected for analysis during each running period. The WR-1 tests (Test 4 and Test 5) were run for 120,000 cycles without interval at a rotational speed of 200 rpm, a contact pressure of 850 MPa, and two creepages of 0.91% and 9.43%.

3.2. Results

3.2.1. Wear rate

Fig. 6 shows the friction coefficient (COF) of the SUROS and WR-1 tests. Clearly, the COF is higher at increased levels of creepage. After 40,000 cycles on each test, when the creepage in the SUROS tests was reduced to 0%, the COF sharply decreases to about 0, as would be

Table 2
Test conditions.

Test No.	Test rig	Driving material	Driven material	Contact pressure/MPa	Creepage/%	Disc speed/rpm	Measurement intervals	Notes
1	SUROS	R260	R260	1500	1.5	400	0–40,000 at 5000 cycle intervals; 40,000–40,500 at 500 cycle intervals (0% slip)	
2	SUROS	R260	R260	1500	1.5	400	0–40,000 at 5000 cycle intervals; 40,000–43,000 at 500 cycle intervals (0% slip)	Repeat of test 1
3	SUROS	R260	R260	900	3	400	0–40,000 at 5000 cycle intervals; 40,000–43,000 at 500 cycle intervals (0% slip)	
4	WR-1	C-class	C-class	850	0.91	200	120,000 cycles without interval	
5	WR-1	C-class	C-class	850	9.43	200	120,000 cycles without interval	

The mass and surface images of discs during the tests were taken using electronic balance (JA4103, accuracy: 0.0001 g) and scanning electron microscope (SEM) (Phenom Pro-SE, Netherlands) respectively. The cross sections were cut along the rolling direction after tests, and prepared for optical microscope (OM) (KEYENCEVHX-6000, Japan) and SEM observations by standard metallographic procedures. The hardness as a function of the depth was measured using a Vickers hardness instrument (MVK-H21, Japan) with the load of 0.49 N (HV_{0.05}) for 10 s dwell time.

expected.

The evolution of wear rate with cycles in the SUROS tests is presented in Fig. 7. As the number of test cycles increases, the wear rates of both discs increase rapidly first, and then stabilize. Interestingly, in each condition, the driving disc is worn more severely than the driven disc, and the wear rate of the driving disc is almost twice that of the driven disc. After 40,000 cycles, when the creepage in the SUROS tests reduces to 0%, a sharp increase in wear rate can be seen within the first 1000 cycles. This may be related to the surface damage, which will be explained in detail below.

Fig. 8a presents the wear rate of the WR-1 tests. Similar to the results of the SUROS tests, the wear rate of the driving disc is significantly higher than that of the driven one. The average values of wear rates in the two tests as a function of $T\gamma/A$ are shown in Fig. 8b. Both driving and driven discs tend to increase with $T\gamma/A$. At the same contact conditions, the wear rates of driving discs are generally higher than that of driven discs.

3.2.2. Worn surface

Fig. 9 shows the evolution of the worn surface with the number of

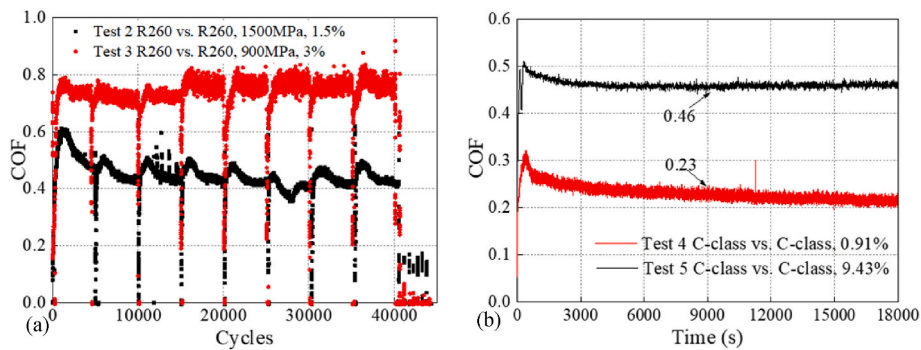


Fig. 6. Friction coefficient (COF): (a) SUROS tests; (b) WR-1 tests.

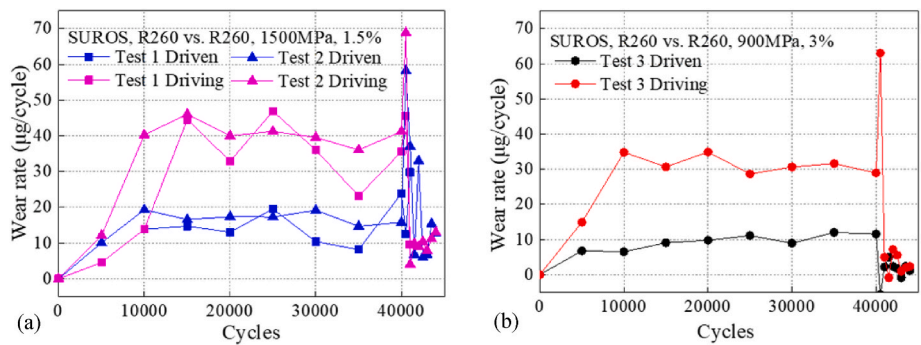


Fig. 7. Wear rate of SUROS tests: (a) Test 1 and Test 2 (1500 MPa, 1.5%); (b) Test 3 (900 MPa, 3%).

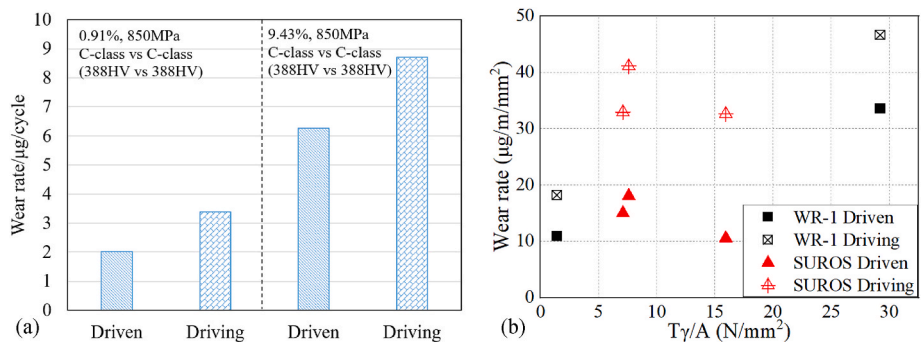


Fig. 8. (a) Wear rate of WR-1 tests; (b) Wear rates as a function of $T\gamma/A$.

cycles in SUROS Test 2 (R260 vs. R260, 1500 MPa, 1.5%). The worn surface of the driven disc is dominated by fatigue damage. Meanwhile, as the number of cycle increases, the surface damage increases. Specifically, the worn surface changes from slight flake and ratcheting within 10,000 cycles to severe flake in 40,000 cycles. When the creepage suddenly disappears after 40,000 cycles, the surface flake damage is reduced. Concerning the driving disc, the worn surface is typified by tribo-chemical reaction and abrasion. Similar to the driven disc, the surface damage of the driving disc increases with cycles. Within the first 10,000 cycles, the worn surface is dominated by metal oxide lamella and ratcheting. As the test progresses, metal oxide lamella, flakes and ploughing can be observed on the worn surface of the driving disc. When the creepage is reduced to 0%, the surface damage gradually transforms to fatigue flakes, which is similar to the driven disc.

The damage mechanisms of the driven and driving discs for Test 3 (not given here) are similar to that in Fig. 9. And the splitting off of the flakes from the surface can explain the sharp increase in wear rate (see Fig. 7) within the first 1000 cycles of 0% creepage. The drop to 0% creepage meant that rather than shearing and growing, the flakes were

subjected to a fatigue process that led to them breaking away at their “roots”. With a further increase in cycles, wear rates of both discs were significantly reduced. With no shear, flakes were no longer being formed. The wear past the removal of the flakes must have been due to mechanism such as abrasion or adhesion rather than ratcheting.

The worn surfaces of the driven and driving discs for WR-1 tests are presented in Fig. 10. Similar to the results of the SUROS tests (Fig. 9), the worn surfaces of the driven discs showed mainly fatigue damage such as flakes (Fig. 10a,c), while numerous oxide lamella composing of adhered metal debris (Fig. 10b,d) can be seen on contact surfaces of the driving discs. Meanwhile, as the creepage increases, the worn surface damage increases. At a creepage of 9.43%, ploughing and large pieces of adhered debris are visible on the driving disc, as shown in Fig. 10d.

Consequently, the surface damage of the driving and driven discs in the SUROS and WR-1 tests is consistent with previous studies [6,13,14], i.e., the driving disc is dominated by tribo-chemical wear, while the driven one is generally by fatigue and abrasion.

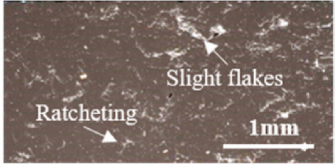
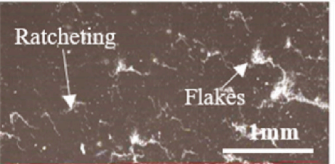
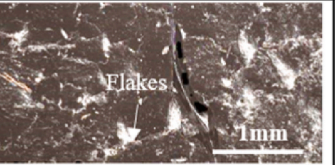
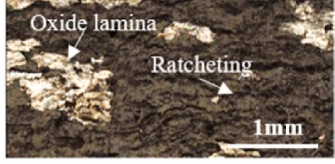
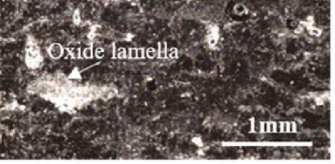
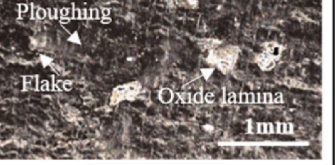
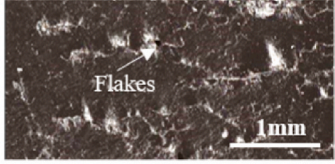
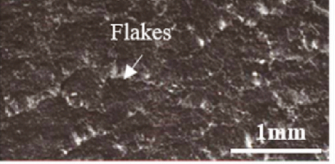
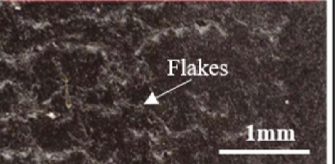

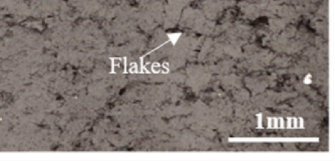
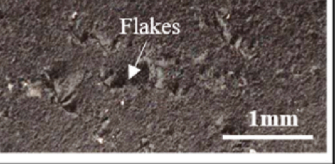
Cycles	5000	10000	30000
Driven disc			
Driving disc			
Cycles	40000	40500	43000
Driven disc			
Driving disc			

Fig. 9. Worn surface as a function of cycles in SUROS Test 2 (R260 vs. R260, 1500 MPa, 1.5%).

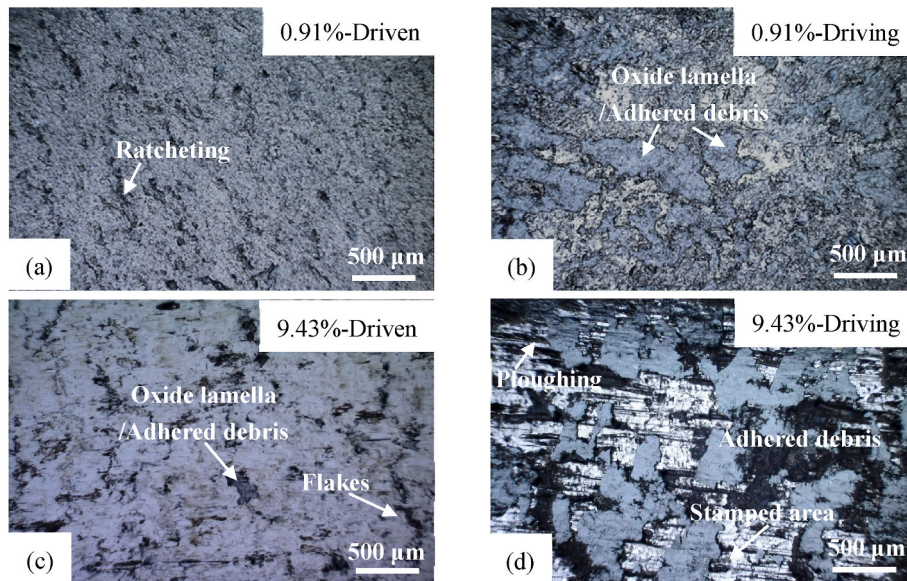


Fig. 10. Worn surfaces in WR-1 tests: (a) Driven disc and (b) Driving disc at the creepage of 0.91%; (c) Driven disc and (d) Driving disc at the creepage of 9.43%.

3.2.3. Plastic deformation and strain hardening

OM and SEM were used to observe the microstructure of the deformation layer of the driven and driving discs for WR-1 tests, as shown in Fig. 11. At a creepage of 0.91%, the plastic flow of the driving disc is more severe and the deformation thickness is deeper than that of the driven disc, see Fig. 11a and b. Meanwhile, the deformed structure of the driven disc is dominated by compression deformation, while compression and shear deformation coexist on the surface structure of the driving disc, and obvious plastic flow can be seen in Fig. 11b. The

difference in deformation indicates that during the contact process, the stress state on the surfaces of two discs is different, and the driving disc may experience a different stress state.

When the creepage was increased to 9.43%, the shear stress on the contact interface increased sharply. Therefore, both discs underwent significant shear deformation. At this point, the thickness of the deformation and the microstructure of the two discs are similar, see Fig. 11c and d. It should be noted that some scattered third-body adhesion layer (formed by the adhesion debris in Fig. 10d) is observed on the surface of

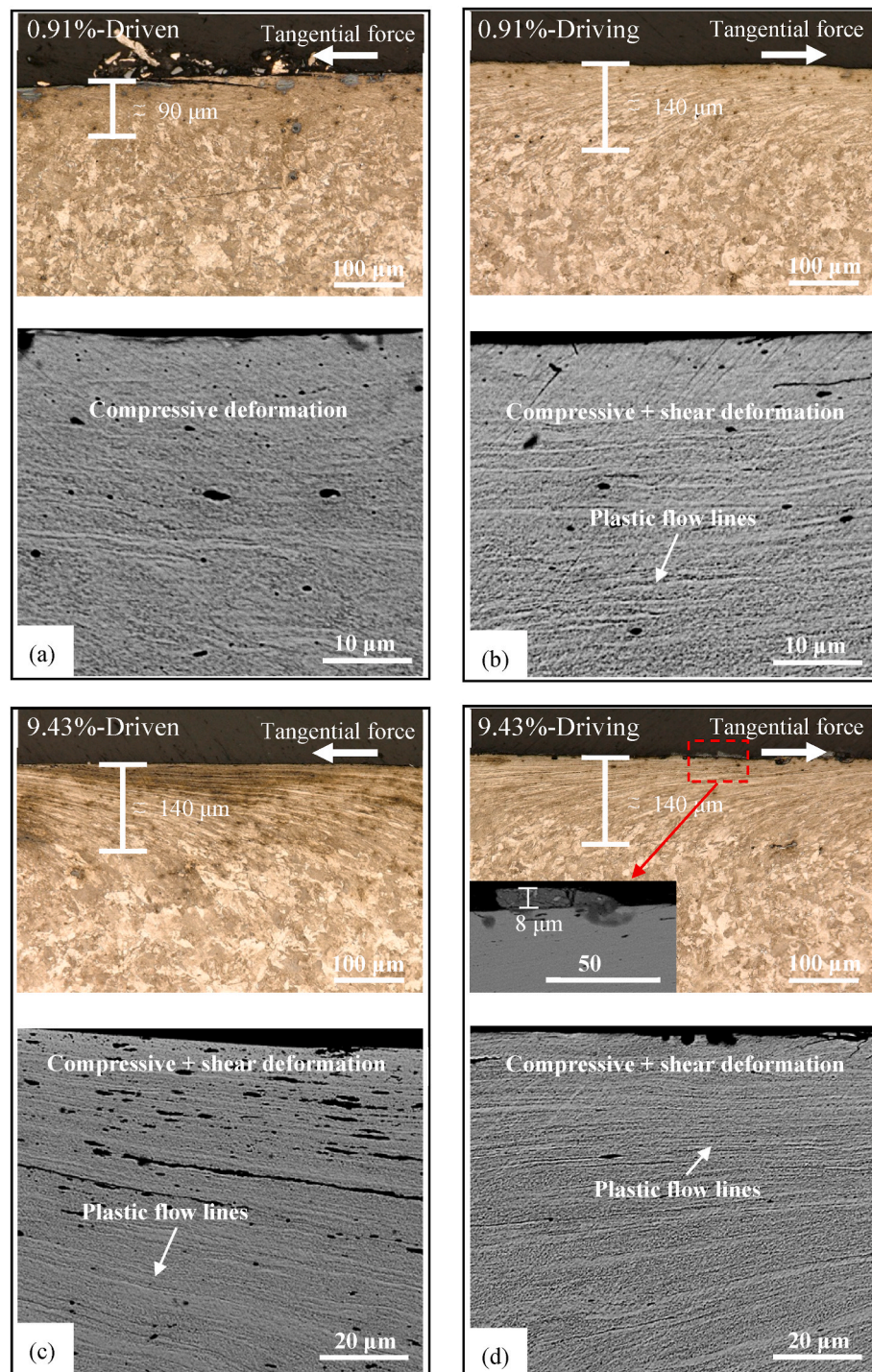


Fig. 11. Plastic deformation in WR-1 tests: (a) Driven disc and (b) Driving disc at the creepage of 0.91%; (c) Driven disc and (d) Driving disc at the creepage of 9.43%.

the driving disc, as shown in Fig. 11d. The formation of the third body layer is related to the thermal effect under the condition of large creepage [21,22].

It is well known that the accumulation of plastic deformation will produce strain hardening. Figs. 12 and 13 present the sub-surface hardness profiles with the depth from the surface in the SUROS and WR-1 tests, respectively. The hardness of the driven and driving discs decrease with the depth from the surface. Meanwhile, near the contact surface, the hardness of the driven disc is higher than that of the driving one for the two series of tests, even though the hardness of the outermost

surface for the driven disc was not measured in Test 3 (Fig. 12b). Therefore, the lower hardness for the driving discs can partly explain its higher wear rates, see Figs. 6 and 7.

At the same depth from the surface, the hardness of the two discs at a higher creepage (Figs. 12b and 13b) are lower than those at low creepage conditions (Figs. 12a and 13a). Similar phenomena have been observed in other studies [23,24]. These can be explained by a mixed mechanism of dynamic softening and strain hardening [25]. A high temperature would be reached at the contact surface of discs at the large creepage conditions. Sometimes it could induce the refined ferrite grains

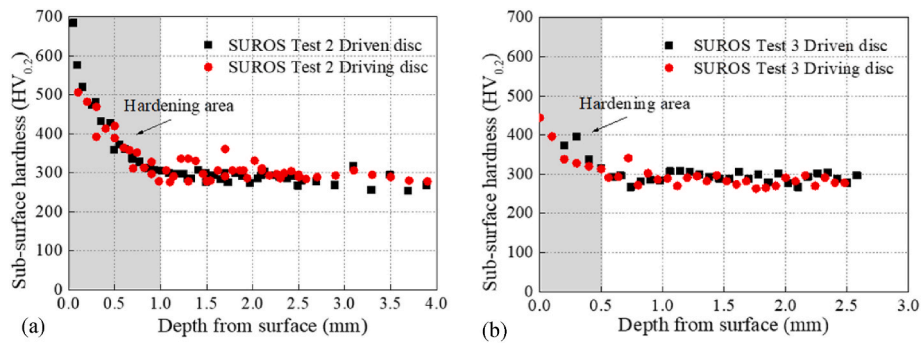


Fig. 12. Hardness profiles for SUROS tests: (a) Test 2 (1500 MPa, 1.5%); (b) Test 3 (900 MPa, 3%).

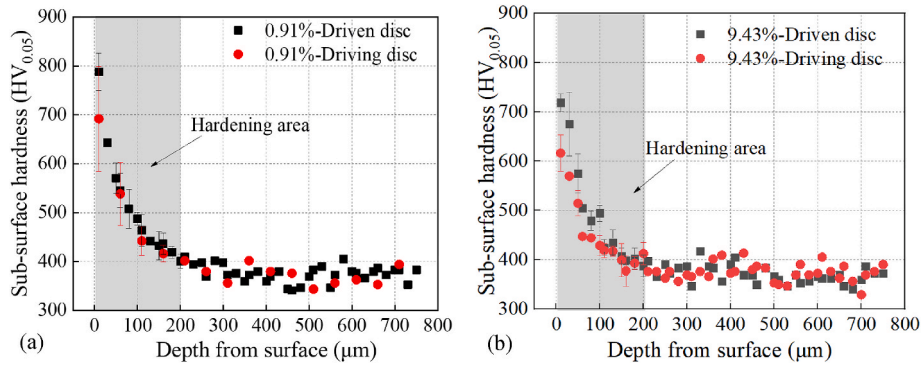


Fig. 13. Hardness profiles for WR-1 tests: (a) Test 4 (0.91%); (b) Test 5 (9.43%).

to recover and soften, resulting in opposing simultaneous effects of hardening and softening during severe deformation.

3.2.4. Fatigue cracking

Fig. 14 presents the SEM images of fatigue cracks on driven and driving discs in WR-1 tests. At the creepage of 0.91%, fatigue cracks of driven and driving discs propagate along the plastic flow at a small

angle. Due to the lower plastic flow of the driven disc, the tip of the fatigue crack is prone to blunt at the kinking microstructure [9,26], as shown in Fig. 14a. Similarly, the fatigue cracks of the driven disc grow along plastic flow at a creepage of 9.43%. Interestingly, branching and joining of fatigue cracks are visible on the driving disc, and then surface damage including spalling and ploughing are formed on the surface, see Fig. 14b,d.

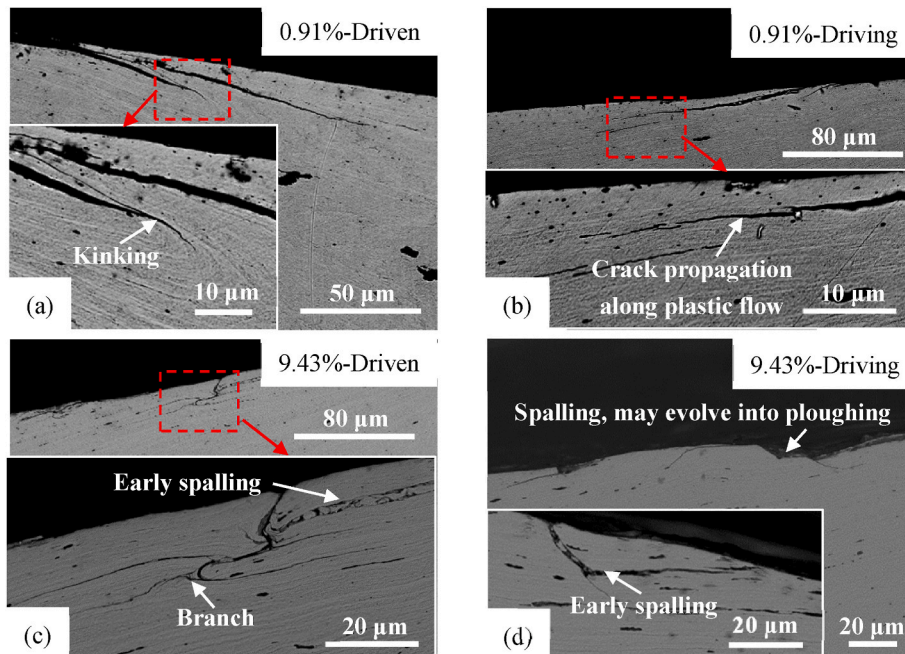


Fig. 14. Fatigue crack morphology in WR-1 tests: (a) Driven disc and (b) Driving disc at the creepage of 0.91%; (c) and (d) Driving disc at the creepage of 9.43%.

Corresponding to its surface damage (Fig. 10), the branching and the change of propagation direction for cracks may be caused by the increase in contact stress induced by the roughness. For example, at high creepage, metal debris was drawn into the contact interface and tended to adhere on the driving disc. The roughness would be changed, which may cause the contact stress to deviate from the assumed Hertzian (smooth) to one with a peak at the exact moment when the debris is in the contact [27].

The fatigue crack size, including crack growth length, angle and depth, were measured and analysed, see Table 3 and Fig. 15. One sample from each test condition was used for the statistical analysis in Table 3 and Fig. 15. The number of cracks on each disc is different due to the different degree of fatigue damage under varying creepage and driving modes. Meanwhile, it is difficult to obtain the same crack numbers in the process of sampling and observing. Therefore, to better characterize fatigue cracks, three small pieces of about 1 mm length were taken from each disc and each piece was separated by 120° from the others. All cracks in the three small pieces were measured and counted. For each disc 40–80 fatigue cracks were analysed. Detailed information of the sampling method can be found in Ref. [11]. At the creepage of 0.91%, similar length and angle distributions of fatigue cracks are observed for the driving and the driven discs. In contrast, at high creepage condition, the driven disc possesses fewer, but generally longer fatigue cracks, as shown in Fig. 15a. It is related to the tribo-chemical wear mechanism of the driving disc and the formation of ploughing and a third-body layer on the worn surface (Fig. 10d) at this condition. Therefore, at the condition of high creepage, the wear and damage mechanism of the two discs is complicated, and it is affected by factors such as contact temperature and wear mechanism.

4. Discussion

4.1. The influence mechanism of driving modes

This work analysed numerous wear results in previous twin disc studies, which were performed under two driving modes (i.e., wheel was run driving - acceleration, rail was run driving - braking). The wear responses for the same wheel-rail pairs (H_R/H_W) differed under different driving conditions. Meanwhile, the surface damage of wheel and rail material indicated that the wear mechanisms for the driving and driven discs were different, and tribo-chemical wear usually occurred on the driving disc. This evidence showed that the driving mode does have an important impact on the wear and damage behaviour of wheel and rail.

Subsequently, the SUROS and WR-1 twin disc rigs were used to perform new tests where the same material pairs were used. The worn surfaces (Figs. 9 and 10) for the driving and driven discs were similar to the previous results [6,13,14], specifically, oxidized metal debris was adhered to the driving disc, and the driven disc was mainly fatigue dominated by flakes. Interestingly, all the tests found that the wear rate of the driving disc was significantly higher than that of the driven disc. In SUROS tests, the value for the driving disc was even 2–3 times that of the driven disc. Although the driving disc does run more cycles than the driven one due to the creepage, such a large difference in wear rates should not be caused by a low creepage of 1.5% or 3%.

The potential influence mechanism of driving modes on wear and damage are as follows:

(1) Hardness

Deters et al. [6] believed that the main reason for the difference in wear rates of wheel and rail between the two driving conditions is the post-test hardness, and the higher post-test hardness resulted in a lower wear rate. It was also found in SUROS and WR-1 tests that the hardness near the surface of the driving disc with high wear rate was lower than that of the driven disc. Although very consistent results were observed, the reason for this difference in work hardening is still unclear.

(2) Formation mechanism of metal debris

Flakes propagated and then split off from the surface during the cyclic loading, forming metal debris, which in turn caused wear. Therefore, the wear mechanism would be closely related to the formation mechanism of debris. The difference in morphology features of worn surfaces between the driving and driven discs (Figs. 4, 9 and 10) indicated the different formation mechanisms of metal debris theoretically, i.e., how the flakes break away. However, the debris collected in these tests was a mixture of splitting off from both driving and driven discs, and it is hard to distinguish which debris was broken from which disc. Therefore, it is necessary to systematically study the fracture process of the metal debris by improving tests and collecting the debris of the driving and driven discs respectively.

(3) Stress state

Theoretically, the stress states differ in driving and driven discs, and this can be inferred from the different deformation levels and hardening rates between the two discs (Figs. 11–13). Deters et al. [6] believed that the driving roller was exposed to lower stresses, resulting in a lower surface hardness. However, that could not explain its higher wear rates, meanwhile, the corresponding modelling of stress distribution was not carried out.

The contact process of the twin disc test is similar to that of differential speed rolling, which is a commonly used method for producing thin metal plates. Due to the difference in the speed of the two working rollers, a cross shear zone with opposite friction force at upper and lower surface of the metal plate appears [28,29], as shown in Fig. 16a. It was found through experiments and finite element analysis that the lower surface of the plate (in contact with the faster roller) exhibited a larger equivalent strain and a higher temperature. If the thickness of the plate was extremely thin, the differential speed rolling system can be ideally considered as a twin disc rolling. Similarly, the strain near the surface of the driving disc in the twin disc test should be greater, and the temperature should be higher as well. This explanation is supported by Zhou et al. [30]. If taking the debris layer as the thin plate in Fig. 16a, the material flow and the temperature rise near the faster disc will be higher. When the temperature near the faster surface is high enough, it will promote the debris to adhere on the disc surface due to the diffusion of oxides [31–33]. As a result, the broken flakes would be more easily adhered to the surface of the driving disc, as shown in Fig. 16b.

In addition, particles such as debris entering the contact interface would increase the roughness and stress. Therefore, subsequent simulation research on the contact stress between the two discs during the action of the debris or the third body layer will be helpful to understand the wear mechanism better.

Table 3

The size statistics of fatigue cracks of driven and driving discs in WR-1 tests.

Creepage	Sample	Ave. Depth (μm)	Max. Depth (μm)	Ave. Length (μm)	Max. Length (μm)	Ave. Degree (°)	Max. Degree (°)
0.91%	Driven	12.1 ± 5.9	30.1	87.7 ± 40.5	240.2	8.4 ± 3.3	18.2
	Driving	9.5 ± 6.9	29.1	87.1 ± 57.7	267.3	6.8 ± 3.4	18.1
9.43%	Driven	15.5 ± 8.0	31.2	116.6 ± 58.8	259.7	8.2 ± 3.4	21.2
	Driving	7.1 ± 3.5	19.7	52.0 ± 27.9	154.2	8.8 ± 3.9	24.1

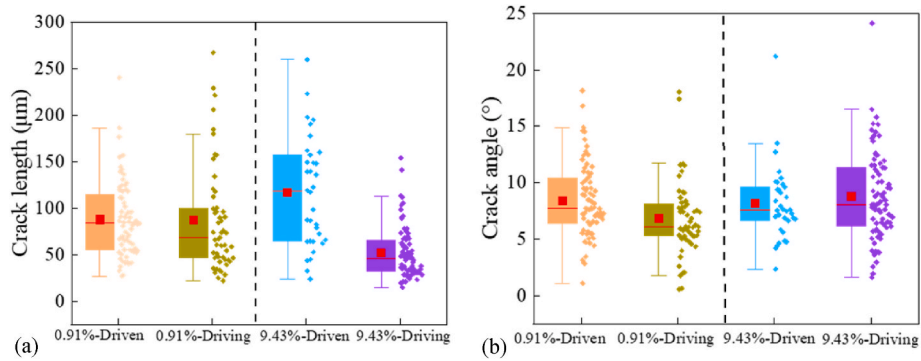


Fig. 15. Box plots of fatigue crack length and angle for driven and driving discs in WR-1 tests: (a) Crack length; (b) Crack angle.

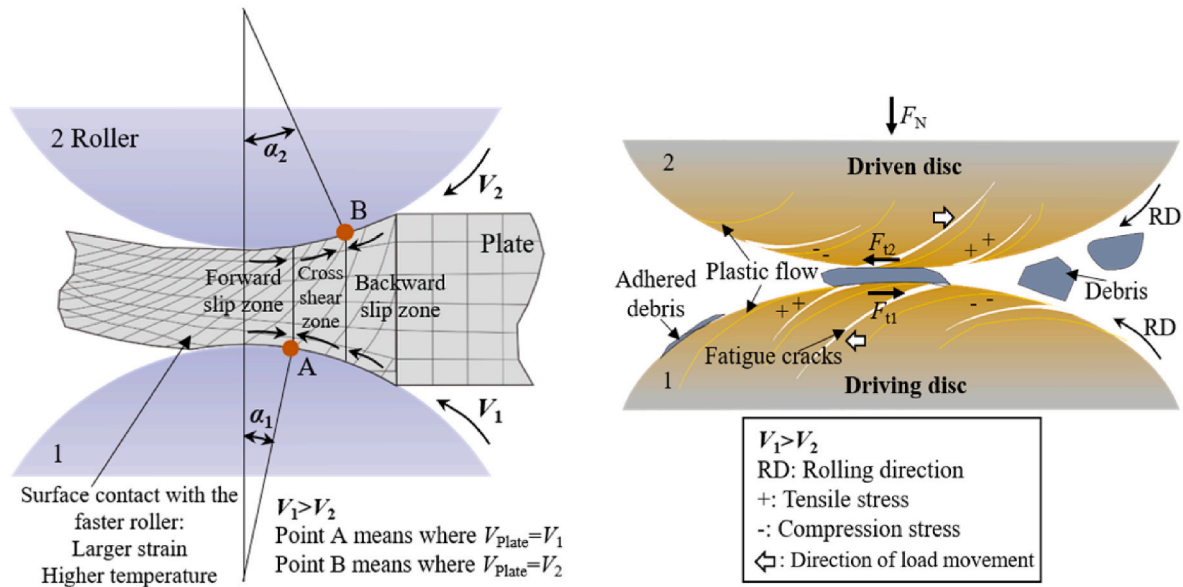


Fig. 16. Schematic diagrams: (a) differential speed rolling [28,29]; (b) twin disc test.

4.2. Other issues worth considering

(1) Materials and properties

It was found in both SUROS and WR-1 tests that the wear rate of the driving disc was significantly higher than that of the driven disc when using the same material. However, a similar phenomenon was not found in previous studies [9,10] in which the same material pair (CL60 wheel and U75V rail) was used while simulated different driving modes, see Fig. 2. The data analysis of previous studies (see Section 2) showed that whether the wheel or the rail was run driving, wheels wore more than rails (even if H_R/H_W was close to 1), and the W_W/W_R values was related to H_R/H_W . Although these were different materials with varying microstructure and hardness, which indicates that these properties are the main factors affecting wear and damage behaviour. Wheel materials generally have proeutectoid ferrite and lamellar pearlite structures, while rail steels are mainly lamellar pearlite. The proeutectoid ferrite with low yield limit is prone to grow cracks. During the cyclic loading, the ferrite deformed to form plastic flow lines, which favoured the propagation of cracks [34–36]. These fatigue cracks broke from the surface, and then debris was formed and wear occurred. Therefore, the wear rate of wheel materials with more proeutectoid ferrites is generally higher than that of rail materials. In previous studies [9,11], when rails were run driving, the rail wear rates may also increase as the new tests in Section 3.1, but the final values were still lower than the wheel wear

rates. Therefore, for the optimization study of material matching in the future, it is necessary to analyze the wear and fatigue damages of wheel-rail pairs under the two driving modes.

(2) Simulation conditions

The WR-1 tests results showed that the worn surface of the driving disc was more likely to adhere metal debris at higher creepage condition, and a third body layer made up of this debris would be formed in severe cases (enhancing the layer already present made up of oxides). The third body layer would affect the traction coefficient, thereby affecting wear and fatigue of wheel and rail [22]. Besides, particles such as metal debris entering the contact interface will increase the roughness and stress. More importantly, the increase in the temperature of the wheel-rail interface at high creepage conditions could affect the damage behaviour as well. Therefore, the damage mechanism under the two driving conditions is related to the simulation conditions, and it is more complicated in severe cases.

5. Conclusions

A review of existing twin disc work on the wear and damage of wheel material and rail material under two conditions where the wheel material was run driving and driven was carried out. There was a consensus on wear mechanism: the driven disc mainly experienced fatigue and

abrasion mechanisms, while the driving one more typified suffered tribo-chemical reaction and fatigue. Besides, wheel materials were generally worn more than rail materials under the both driving cases. Meanwhile, the wear ratio (W_W/W_R) was closely related with material matching behaviour (H_R/H_W).

New tests using the same material for the two discs were then performed on SUROS and WR-1 rigs. The wear rate of the driving disc was significantly higher than that of the driven one. At a low creepage of 1%, compared with the driven disc, the driving one presented a stronger plastic flow and lower work hardening. With increasing creepage, the oxide lamella and ploughing were obvious on the worn surface of driving disc, resulting in the shorter fatigue cracks.

Analysis of the potential causes for the difference in wear behaviours between the driving and driven discs was carried out. A series of future research targets were identified: the hardening mechanism; the formation mechanism of metal debris; the stress distribution; the microstructure and properties of materials; the varying work conditions.

This work has confirmed the influence of driving modes on the wear and damage behaviour of the materials in the twin disc test, and provided some important new data on wear trends at different driving conditions that will be helpful in the subsequent simulation work.

Declaration of competing interest

The authors declare that they have no known competing financial interests or personal relationships that could have appeared to influence the work reported in this paper.

Data availability

Data will be made available on request.

Acknowledgements

The publication was written with support of Virtual Vehicle Research GmbH in Graz, Austria. The authors would like to acknowledge the financial support within the COMET K2 Competence Centers for Excellent Technologies from the Austrian Federal Ministry for Climate Action (BMK), the Austrian Federal Ministry for Digital and Economic Affairs (BMDW), the Province of Styria and the Styrian Business Promotion Agency (SFG). The Austrian Research Promotion Agency (FFG) has been authorised for the programme management. They would furthermore like to express their thanks to their supporting industrial and scientific project partners Siemens Mobility GmbH, voestalpine Rail Technology GmbH and the University of Sheffield. The work was also supported by National Natural Science Foundation of China (Nos. 51975489, 52205239), Sichuan Science and Technology Program (2022NSFSC1903), the Fundamental Research Funds for the Central Universities (J2022-033) and EPSRC programme grant: Friction the tribology enigma (EP/R001766/1). For the purpose of open access, the author has applied a Creative Commons Attribution (CC BY) license to any Author Accepted Manuscript version arising.

References

- [1] Y. Zhu, W.J. Wang, R. Lewis, W. Yan, S.R. Lewis, H. Ding, A review on wear between railway wheels and rails under environmental conditions, *J. Tribol.* 141 (2019), 120801.
- [2] E. Butini, L. Marini, M. Meacci, E. Meli, A. Rindi, X.J. Zhao, W.J. Wang, An innovative model for the prediction of wheel - rail wear and rolling contact fatigue, *Wear* 436 (2019), 203025.
- [3] P. Boyacioglu, A. Bevan, Prediction of Rail Damage Using a Combination of Shakedown Map and Wheel-Rail Contact Energy, *Wear*, 2020, pp. 460–461, 203457.
- [4] R. Lewis, E. Magel, W.J. Wang, U. Olofsson, S. Lewis, T. Slatter, A. Beagles, Towards a standard approach for the wear testing of wheel and rail materials, *Proc. Inst. Mech. Eng. - Part F J. Rail Rapid Transit* 231 (7) (2017) 760–774.
- [5] W.J. Wang, R. Lewis, B. Yang, L.C. Guo, Q.Y. Liu, M.H. Zhu, Wear and damage transitions of wheel and rail materials under various contact conditions, *Wear* 362–363 (2016) 146–152.
- [6] L. Deters, M. Proksch, Friction and wear testing of rail and wheel material, *Wear* 258 (2005) 981–991.
- [7] R. Lewis, P. Christoforou, W.J. Wang, A. Beagles, M. Burstow, S.R. Lewis, Investigation of the influence of rail hardness on the wear of rail and wheel materials under dry conditions (ICRI Wear Mapping Project), *Wear* 430–431 (2019) 383–392.
- [8] R. Lewis, R.S. Dwyer-Joyce, Wear mechanisms and transitions in railway wheel steels, *Proceedings of the Institution of Mechanical Engineers, Participant J.: Journal of Engineering Tribology* 218 (6) (2004) 467–478.
- [9] Y. Hu, L. Zhou, H.H. Ding, G.X. Tan, R. Lewis, Q.Y. Liu, J. Guo, W.J. Wang, Investigation on wear and rolling contact fatigue of wheel-rail materials under various wheel/rail hardness ratio and creepage conditions, *Tribol. Int.* 143 (2020), 106091.
- [10] L.C. Guo, W.T. Zhu, L.B. Shi, Q.Y. Liu, Z.B. Cai, W.J. Wang, Study on wear transition mechanism and wear map of CL60 wheel material under dry and wet conditions, *Wear* 426 (2019) 1771–1780.
- [11] Y. Hu, M. Watson, M. Maiorino, L. Zhou, W.J. Wang, H.H. Ding, R. Lewis, E. Meli, A. Rindi, Q.Y. Liu, J. Guo, Experimental study on wear properties of wheel and rail materials with different hardness values, *Wear* (2021), <https://doi.org/10.1016/j.wear.2021.203831>.
- [12] J.W. Seo, S.J. Kwon, H.K. Jun, C.W. Lee, Effects of wheel materials on wear and fatigue damage behaviors of wheels/rails, *Tribol. Trans.* 62 (4) (2019) 635–649.
- [13] W.T. Zhu, L.C. Guo, L.B. Shi, Z.B. Cai, Q.L. Li, Q.Y. Liu, W.J. Wang, Wear and damage transitions of two kinds of wheel materials in the rolling-sliding contact, *Wear* 398–399 (2018) 79–89.
- [14] Y. Hu, C.R. Su, L.C. Guo, Q.Y. Liu, J. Guo, Z.R. Zhou, W.J. Wang, Effect of rolling direction on microstructure evolution of CL60 wheel steel, *Wear* 424 (2019) 203–215.
- [15] J.F. Santa, P. Cuervo, P. Christoforou, M. Harmon, A. Beagles, A. Toro, R. Lewis, Twin disc assessment of wear regime transitions and rolling contact fatigue, *Wear*, in: R400HT-E8 Pairs, 2019, pp. 432–433, 102916.
- [16] R. Lewis, R.S. Dwyer-Joyce, U. Olofsson, J. Pombo, J. Ambrosio, M. Pereira, N. Kuka, Mapping railway wheel material wear mechanisms and transitions, *Proc. Inst. Mech. Eng. - Part F J. Rail Rapid Transit* 224 (3) (2010) 125–137.
- [17] P.J. Bolton, P. Clayton, Rolling-sliding wear damage in rail and tyre steels, *Wear* 93 (1984) 145–165.
- [18] A. Kapoor, D.I. Fletcher, F.J. Franklin, The role of wear in enhancing rail life, 2003, *Proceedings of the 29th Leeds-Lyon Symposium on Tribology* (2003) 331–340.
- [19] D.I. Fletcher, J.H. Beynon, Development of a machine for closely controlled rolling contact fatigue and wear testing, *J. Test. Eval.* 28 (4) (2000) 267–275.
- [20] H. Al-Maliki, A. Meierhofer, G. Trummer, R. Lewis, K. Six, A new approach for modelling mild and severe wear in wheel-rail contacts, *Wear* 476 (2021), 203761.
- [21] G. Donzella, M. Faccoli, A. Mazzù, C. Petrogalli, R. Roberti, Progressive damage assessment in the near-surface layer of railway wheel-rail couple under cyclic contact, *Wear* 271 (2011) 408–416.
- [22] A. Meierhofer, C. Hardwick, R. Lewis, K. Six, P. Dietmaier, Third body layer-experimental results and a model describing its influence on the traction coefficient, *Wear* 314 (2014) 148–154.
- [23] U. Cihak-Bayr, G. Mozdzen, E. Badisch, A. Merstallinger, H. Winkelmann, High plastically deformed sub-surface tribozones in sliding experiments, *Wear* 309 (2014) 11–20.
- [24] Q.Y. Meng, D.Y. Liu, P.T. Liu, X.J. Zhao, R.M. Ren, Effect of rolling-sliding friction on microstructure of U75V steel, 04, *J. Dalian Jiaot. Univ.* 37 (2016) 100–104 (in Chinese).
- [25] B. Eghbali, Study on the ferrite grain refinement during intercritical deformation of a microalloyed steel, *Mater. Sci. Eng., A* 527 (2010) 3407–3410.
- [26] O.P. Datsyshyn, H.P. Marchenko, A.Y. Glazov, On the special angle of surface cracks propagation in the railway rail heads, *Eng. Fract. Mech.* 206 (2019) 452–462.
- [27] A. Kapoor, F.J. Franklin, S.K. Wong, M. Ishida, Surface roughness and plastic flow in rail wheel contact, *Wear* 253 (1–2) (2002) 257–264.
- [28] T. Zhang, L. Li, S.H. Lu, J.B. Zhang, H. Gong, Comparisons of flow behavior characteristics and microstructure between asymmetrical shear rolling and symmetrical rolling by macro/micro coupling simulation, *Journal of Computational Science* 29 (2018) 142–152.
- [29] Y.H. Ji, J.J. Park, W.J. Kim, Finite element analysis of severe deformation in Mg–3Al–1Zn sheets through differential-speed rolling with a high speed ratio, *Mater. Sci. Eng.* 454–455 (2007) 570–574.
- [30] L. Zhou, H.H. Ding, Z.Y. Han, C.M. Chen, Q.Y. Liu, J. Guo, W.J. Wang, Study of Rolling-Sliding Contact Damage and Tribo-Chemical Behaviour of Wheel-Rail Materials at Low Temperatures, *Engineering Failure Analysis*, 2022, 106077.
- [31] H. Kato, K. Komai, Tribofilm formation and mild wear by tribo-sintering of nanometer-sized oxide particles on rubbing steel surfaces, *Wear* 262 (2007) 36–41.
- [32] A. Dreano, S. Fouvry, G. Guillonnet, Understanding and formalization of the fretting-wear behavior of a cobalt-based alloy at high temperature, *Wear* 452–453 (2020), 203297.
- [33] M.H. Attia, A.D. Pannemaeker, G. Williams, Effect of Temperature on Tribo-Oxide Formation and the Fretting Wear and Friction Behavior of Zirconium and Nickel-Based Alloys, *Wear*, 2021, 203722.

- [34] J. Garnham, C. Davis, The role of deformed rail microstructure on rolling contact fatigue initiation, *Wear* 265 (2008) 1363–1372.
- [35] Y. Hu, L. Zhou, H.H. Ding, R. Lewis, Q.Y. Liu, J. Guo, W.J. Wang, Microstructure evolution of railway pearlitic wheel steels under rolling-sliding contact loading, *Tribol. Int.* 154 (2021), 106685.
- [36] G. Trummer, C. Marte, P. Dietmaier, C. Sommitsch, K. Six, Modeling surface rolling contact fatigue crack initiation taking severe plastic shear deformation into account, *Wear* 352–353 (2016) 136–145.